EUROPEAN ORGANIZATION FOR NUCLEAR RESEARCH

CERN-EP/84-170
18 December 1984

CONTRIBUTION OF HARD QCD INTERACTIONS TO $p\bar{p}$-pp TOTAL INELASTIC CROSS-SECTION DIFFERENCE AT THE CERN ISR ENERGIES

V. Cavasinni, T. Del Prete, M. Morganti and R. Tripiccione

Dipartimento di Fisica dell'Università
and INFN, Pisa, Italy

and

CERN, Geneva, Switzerland

ABSTRACT

We have performed a first-order QCD calculation to evaluate a possible contribution of large-Q^2 scattering to $p\bar{p}$/pp total inelastic cross-section difference at the CERN Intersecting Storage Rings (ISR). We found that at $\sqrt{s} = 31$ GeV and for $Q^2 \geq 6$ GeV^2 there is a small (a few microbarns, but definitely not 0) difference in favour of the $p\bar{p}$ reaction. This effect is confined to the central rapidity region ($|y| \leq 1$) and diminishes with increasing centre-of-mass energy.

(Submitted to Physics Letters B)

1. INTRODUCTION

Recent experiments performed at the CERN Intersecting Storage Rings (ISR) have shown that the proton–antiproton/proton–proton total cross-section difference, although diminishing, is still of the order of 1 mb over the ISR energy range [1, 2]. The origin of this difference can be accounted for by the Regge-pole model via the dominant contribution of the ϱ and ω trajectories [3].

In the framework of quantum chromodynamics (QCD), it might be expected that quark–antiquark annihilation into quark or gluon pairs would play a more important role in $p\bar{p}$ collisions than it does in pp collisions, yielding a larger two-jet cross-section for the former process. Owing to the balanced quark and antiquark structure functions in the proton and in the antiproton this production would be central in rapidity, i.e. $|y|_{jet} \lesssim 1$. Reference [4] reports a measurement of $p\bar{p}$ and pp two-particle rapidity correlation at $\sqrt{s} = 31$ GeV. The correlation measured in $p\bar{p}$ collisions is stronger than that in the pp case. The excess of correlation [fig. 1 (taken from ref. 4)] is visible only at $|y| \lesssim 1$, and has a range shorter than the usual range of the two-body correlation ($\Delta y \sim 0.3$ instead of 1). A simple model in which a difference of 0.1–0.2 mb in jet cross-section between $p\bar{p}$ and pp interactions was assumed, reproduces nicely the difference in correlation [4]. These jets were assumed to be centrally produced with an angular dispersion, relative to the jet axis, similar to that measured at low-energy in e^+e^- interactions.

In this paper we will show the results of a QCD calculation of the difference in jet cross-section between $p\bar{p}$ and pp interactions at the ISR energies. This calculation shows that more jets are yielded by $p\bar{p}$ collisions than by pp, and that this difference is mainly present around $y = 0$. However, the difference, which decreases with energy, is only a few microbarns in size, and is therefore quantitatively insufficient to account for the differences in the two-body correlation measured in $p\bar{p}$ and pp interactions.

2. CALCULATION OF THE QCD CROSS-SECTIONS

In QCD, quarks (q) and gluons (g) can interact through eight fundamental processes:

i)	$q_iq_i \rightarrow q_iq_i$	
ii)	$q_i\bar{q}_i \rightarrow q_i\bar{q}_i$	
iii)	$q_i\bar{q}_i \rightarrow gg$	
iv)	$q_i\bar{q}_i \rightarrow q_j\bar{q}_j$	$i \neq j$
v)	$q_iq_j \rightarrow q_iq_j$ $q_i\bar{q}_j \rightarrow q_i\bar{q}_j$	$i \neq j$
vi)	$gg \rightarrow q_i\bar{q}_i$	
vii)	$q_ig \rightarrow q_ig$	
viii)	$gg \rightarrow gg$	

In process (v), $p\bar{p}$ and pp interactions are simply related by a charge-conjugation operation and therefore we do not expect differences. Processes (vi) to (viii) contain gluons in the initial state, and again they do not contribute to the $p\bar{p}$/pp difference.

Process (i) is the interaction between equal particles; thus we expect that it is more frequent in pp than in $p\bar{p}$ scattering. Processes (ii) to (iv) are interactions between particle and antiparticle which are favoured in $p\bar{p}$ scattering.

The QCD differential cross-sections for all the above elementary processes are well known [5].

The choice of the quantity Q^2 relevant to the QCD calculation deserves some care. For process (iv) there is no ambiguity, and in this case we take $Q^2 = \hat{s}$ [$\hat{s}$, $\hat{t}$, $\hat{u}$, are the Mandelstam variables of the elementary quark–(anti)quark interaction]. For processes (i) to (iii) we follow most authors and take

$$Q^2 = 2\hat{s}\hat{t}\hat{u}/(\hat{s}^2 + \hat{t}^2 + \hat{u}^2) \tag{1}$$

The QCD effective coupling constant is $\alpha_s(Q^2) = 12\pi/[25 \ln (Q^2/\Lambda^2)]$, and we assume a cut-off $\Lambda = 0.25$ GeV [6]. In the case of reaction (iv), the cross-section is summed over all the possible quark flavours in the final state.

The valence- and sea-quark structure functions used in the calculation are those parametrized by Buras and Gaemers [7], and we have checked that the results are quite insensitive to any other choice of such parametrization [8].

The rapidity of the jet is related to the fractionary momentum of the two incoming partons x_1 and x_2 and to the $\hat{t}$ of the scattered quark through the formula

$$y = \tfrac{1}{2} \ln [- (x_1/x_2 + x_1^2 s/\hat{t})] . \tag{2}$$

The $p\bar{p}/pp$ difference in cross-section at rapidity y of the scattered quark is calculated by performing the integral

$$d\sigma/dy = \int_0^1 dx_1 \int_0^1 dx_2 \, d\hat{t} \, \delta \{ y - \tfrac{1}{2} \ln [- (x_1/x_2 + x_1^2 s/\hat{t})] \} \, d\sigma/d\hat{t} \, f(x_1) g(x_2) , \tag{3}$$

where $d\sigma/d\hat{t}$ is the QCD cross-section of the elementary subprocess; $f(x_1)$, $g(x_2)$ are the differences in the probability between $p\bar{p}$ and pp for the two incoming partons to carry a fraction x_1 (x_2) of the momentum of the parent nucleon. Integration over $\hat{t}$ eliminates the δ function, and the integral can be computed numerically for those Q^2 (a function of x_1, x_2, and $\hat{t}$) satisfying the condition $Q^2 > Q_0^2$, where Q_0^2 is a lower cut-off. If, on the contrary, Q^2 is lower than Q_0, the cross-section difference is set to 0.

We estimate the uncertainty from the integration procedure to be less than 5%.

3. THE RESULTS

First, we consider $\sigma(p\bar{p}) - \sigma(pp)$ integrated over the full rapidity range (difference between total inelastic cross-sections), and in the reduced interval $|y| \leq 1$ as a function of the cut-off Q_0^2. Figure 2 shows these results at $\sqrt{s} = 31$ GeV. We see that the jet cross-section is larger in $p\bar{p}$ interactions as $Q_0^2 > 3$ GeV^2. This difference reaches the maximum of ~ 4 μb at $Q_0^2 = 6$ GeV^2, and about 2/3 of it is confined at $|y| < 1$.

The same calculation performed at $\sqrt{s} = 63$ GeV is shown in Fig. 3: the Q_0^2 at which the $p\bar{p}$ cross-section becomes larger than the pp one moves toward larger values of Q_0^2 ($Q^2 \sim 9$ GeV^2) compared with the behaviour at $\sqrt{s} = 31$ GeV, and moreover the effect is smaller.

At $\sqrt{s} = 31$ GeV the y-dependence of the difference in the jet cross-section for $p\bar{p}$ and pp reactions is investigated for each interaction type at $Q_0^2 = 6$ GeV^2 (i.e. at the maximum of the difference). The results of the calculation are shown in Figs. 4a to 4d. As expected, the difference for interaction type (i) is negative (dominance of pp jets) whilst it is positive for the three remaining hard interactions. Figure 4e is the algebraic sum of Figs. 4a to 4d. The over-all jet cross-section is larger in $p\bar{p}$ than in pp interactions, and the maximum of the difference peaks at $y = 0$ and falls to 0 at $y \cong 1.3$.

In a way similar to that used for the y-distribution, we have calculated also the difference in transverse momentum distribution between the two reactions, again separately for each process and at $Q_0^2 = 6$ GeV. The results are shown in Figs. 5 at $\sqrt{s} = 31$ GeV and at $|y| < 1$. We see again a negative difference for process (i) and a positive difference for reactions (ii) to (iv). The sharp cut-off of the distribution present in processes (i) to (iii) reflects the choice of Q^2 for these processes [Eq. (1)]. In fact in these cases a lower limit for Q^2 translates directly in a lower limit of p_T. On the contrary, p_T in reaction (iv) is only indirectly affected by the cut-off in Q^2, resulting in a distribution that can extend also at low-p_T values (Fig. 5d). Figure 5e is the algebraic sum of distributions 5a, 5b, 5c.

From Figs. 5 we see that:

a) the jet cross-section in larger in the case of $p\bar{p}$ compared to pp interactions;
b) this excess is due to reaction type (iv), and is broadly distributed around an average p_T of 1.3 GeV (Fig. 5d);
c) reaction types (i) to (iii) provide a jet yield almost equal in $p\bar{p}$ and pp collisions, pp interactions being slightly favoured (Fig. 5e).

4. CONCLUSIONS

The results of our calculation can be summarized as follows:

1) QCD first-order processes at $\sqrt{s} = 31$ GeV slightly favour jet production in $p\bar{p}$ interactions with respect to pp interactions; this production, at moderate p_T ($\sim$ 1.3 GeV/c), originates from a $q\bar{q}$ annihilation process. At higher p_T the contribution from identical particle scattering favours jet production in pp collisions, but the effect is less sizeable than the previous one.
2) The over-all cross-section difference is small ($\sim 4\ \mu$b for $Q_0^2 > 6$ GeV^2), is centred at rapidity $y = 0$, and ranges between -1.3 and 1.3 in rapidity.
3) The $\sigma(p\bar{p}) - \sigma(pp)$ decreases as the centre-of-mass energy increases.

Some of the above features satisfy the requirements needed to explain the stronger correlation measured in $p\bar{p}$ (with respect to pp), i.e. central rapidity production, and transverse momenta similar to those of jets measured in e^+e^- at SPEAR. However, the size of the effect (a few microbarns) is quantitatively too small by a factor of $\sim$ 50 to account for the measured difference in two-body correlation. We therefore conclude that the $p\bar{p}$/pp differences in the two-body correlation—as well as the difference in total cross-sections—have to find an explanation within 'soft' interaction models.

Acknowledgements

We wish to thank K. Konishi for enlightening discussions and R. Petronzio for his careful and critical reading of the manuscript.

REFERENCES

[1] G. Carboni et al., Phys. Lett. **113B** (1982) 87.
M. Ambrosio et al., Phys. Lett. **115B** (1982) 495.
G. Carboni et al., preprint CERN-EP/84-163 (1984).

[2] N. Amos et al., Phys. Lett. **120B** (1983) 460.
N. Amos et al., Phys. Lett. **128B** (1983) 343.

[3] See, for example, the review of J.G. Rushbrooke and B.R. Webber, Phys. Rep. **44** (1978) 1.

[4] V. Cavasinni et al., Z. Phys. **C21** (1984) 299.

[5] B.L. Combridge, J. Kripfganz and J. Ranft, Phys. Lett. **70B** (1977) 234.

[6] M. Althoff et al. (TASSO Collaboration), preprint DESY 84-057 (1984).

[7] A.J. Buras and K.J. Gaëmers, Nucl. Phys. **B132** (1978) 249.

[8] J.F. Owens and E. Reja, Phys. Rev. **D17** (1978) 3003.

Figure captions

Fig. 1: Normalized two-body correlation function $R_2(\eta_1, \eta_2)$ at $\sqrt{s} = 31$ GeV for $-0.36 \leq \eta_1 \leq 0.12$ in $p\bar{p}$ (full points) and pp (open circles) interactions (data taken from ref. [4]).

Fig. 2: Jet cross-section difference at $\sqrt{s} = 31$ GeV between $p\bar{p}$ and pp as a function of the lower cut-off Q_0^2 integrated over the full rapidity range (solid line) and at $|y| \leq 1$ (dashed line).

Fig. 3: Same as Fig. 2 but at $\sqrt{s} = 63$ GeV.

Figs. 4a–d: $p\bar{p}$/pp jet cross-section difference at $\sqrt{s} = 31$ GeV as a function of the jet rapidity and for four QCD processes:

a) $q_i q_i \rightarrow q_i q_i$,

b) $q_i \bar{q}_i \rightarrow q_i \bar{q}_i$,

c) $q_i \bar{q}_i \rightarrow gg$,

d) $q_i \bar{q}_i \rightarrow q_j \bar{q}_j \quad (i \neq j)$.

Fig. 4e: Algebraic sum of the distributions 4a to 4d.

Figs. 5a–d: $p\bar{p}$/pp jet cross-section difference at $\sqrt{s} = 31$ GeV and at $|y| < 1$ as a function of the jet transverse momentum p_T and for the same four QCD processes as in Fig. 4.

Fig. 5e: Algebraic sum of the distributions in 5a, 5b, and 5c.

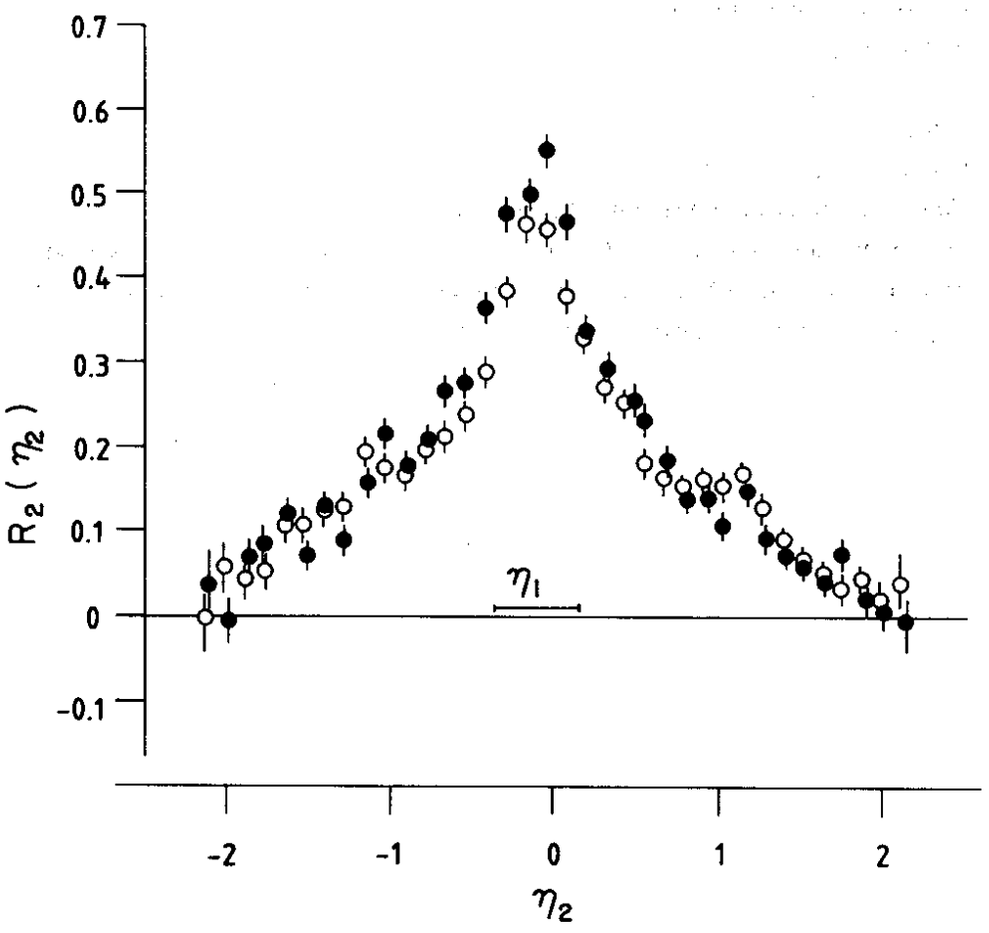

Fig. 1

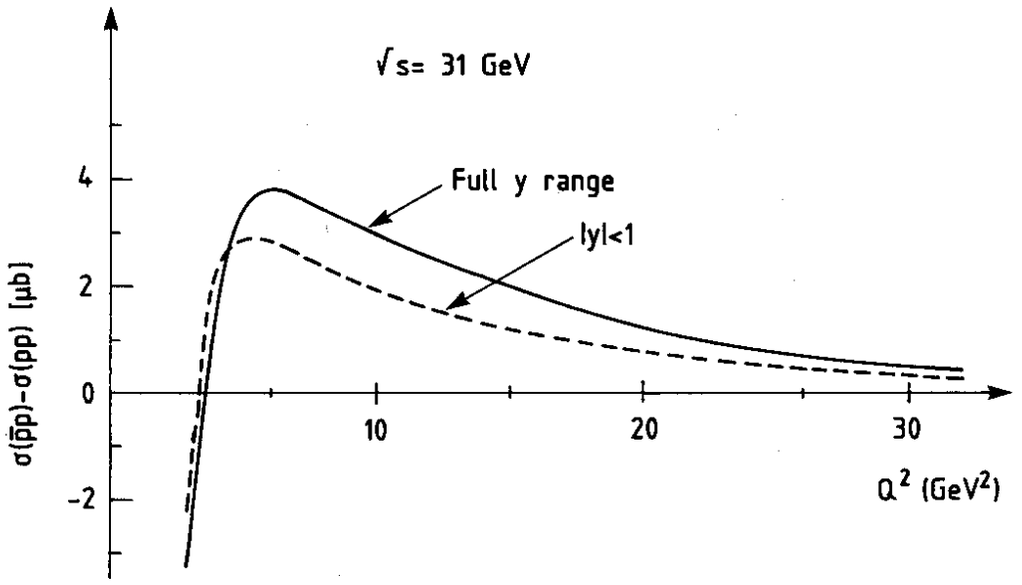
√s= 31 GeV
Full y range
|y|<1
σ(p̄p)-σ(pp) [μb]
4
2
0
-2
10
20
30
Q² (GeV²)

Fig. 2

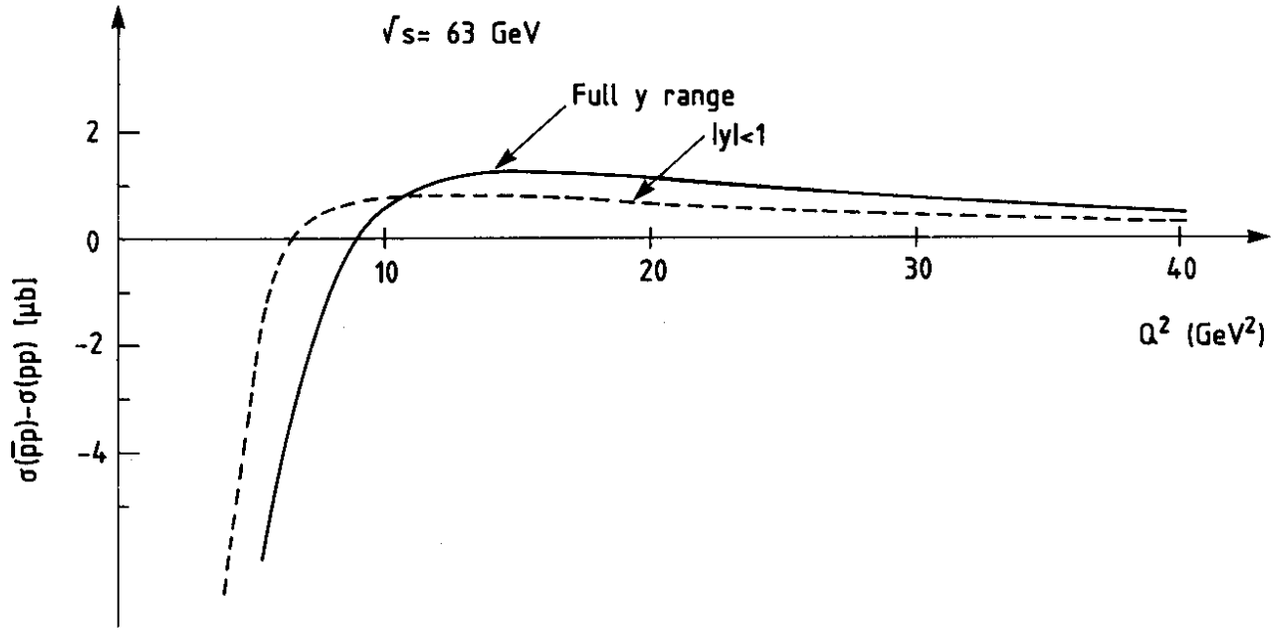
√s= 63 GeV
Full y range
|y|<1
σ(p̄p)-σ(pp) [μb]
2
0
-2
-4
10
20
30
40
Q² (GeV²)

Fig. 3

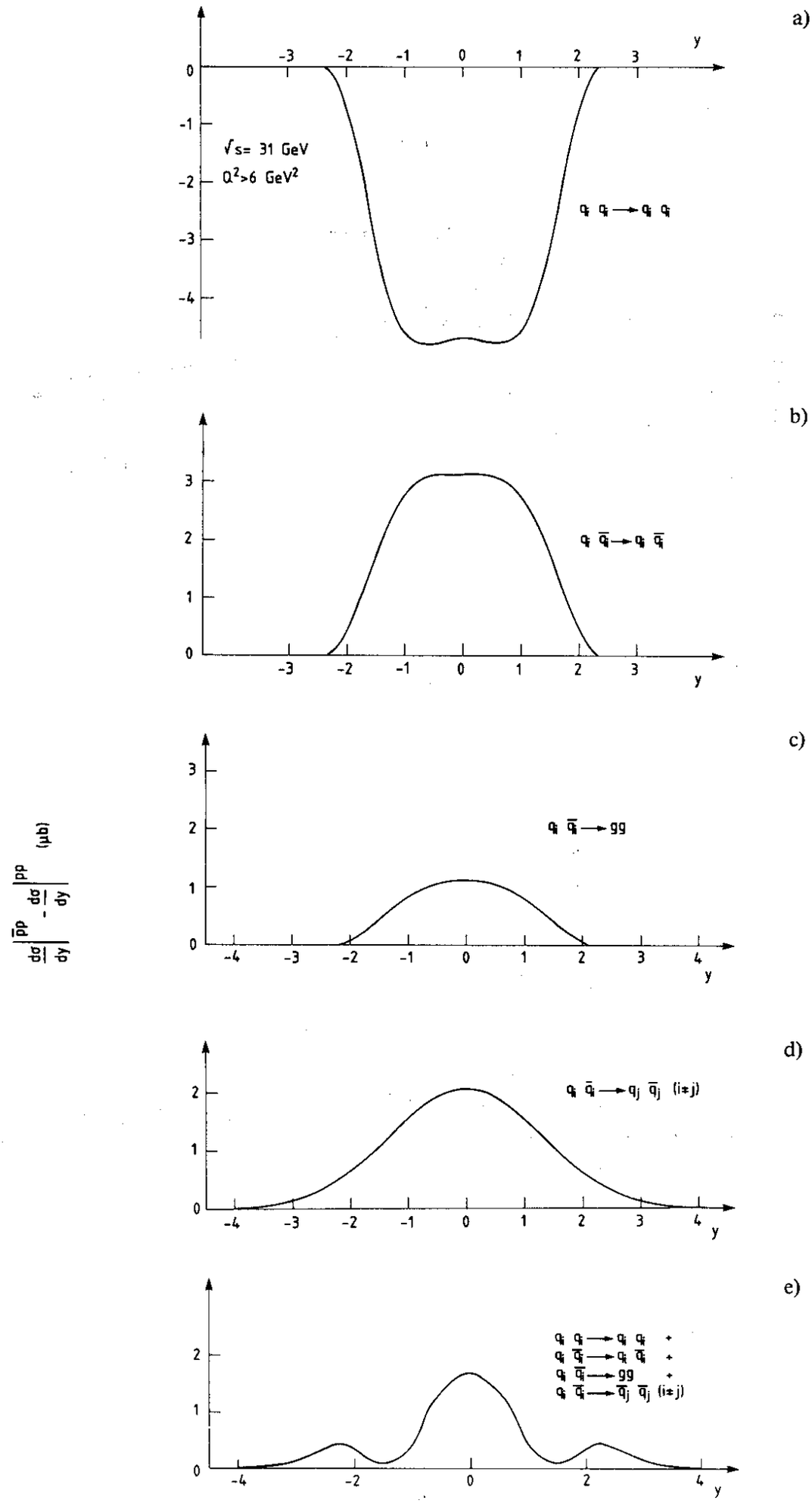
a)
b)
c)
d)
e)
y
$\sqrt{s}$= 31 GeV
Q^2>6 GeV^2
$q_i\ q_i \to q_i\ q_i$
$q_i\ \bar{q}_i \to q_i\ \bar{q}_i$
$q_i\ \bar{q}_i \to gg$
$q_i\ \bar{q}_i \to q_j\ \bar{q}_j$ (i≠j)
$q_i\ q_i \to q_i\ q_i$ +
$q_i\ \bar{q}_i \to q_i\ \bar{q}_i$ +
$q_i\ \bar{q}_i \to gg$ +
$q_i\ \bar{q}_i \to \bar{q}_j\ \bar{q}_j$ (i≠j)
$\frac{d\sigma}{dy}\Big|_{\bar{p}p} - \frac{d\sigma}{dy}\Big|_{pp}$ (μb)

Fig. 4

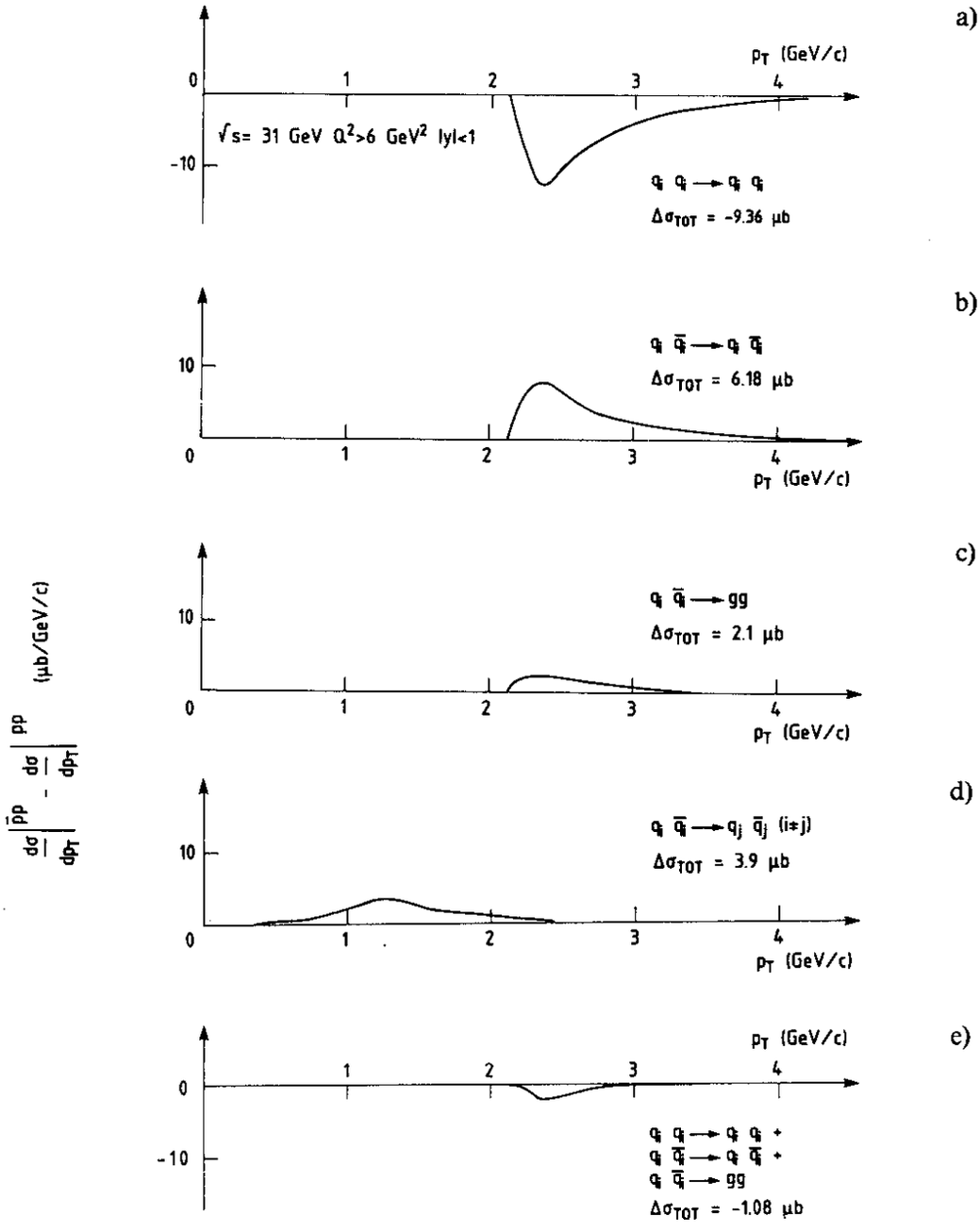
a)
p_T (GeV/c)
0
1
2
3
4
$\sqrt{s}$= 31 GeV Q^2>6 GeV^2 |y|<1
-10
$q_i\ q_i \rightarrow q_i\ q_i$
$\Delta\sigma_{TOT}$ = -9.36 μb
b)
10
0
$q_i\ \bar{q}_i \rightarrow q_i\ \bar{q}_i$
$\Delta\sigma_{TOT}$ = 6.18 μb
c)
$q_i\ \bar{q}_i \rightarrow gg$
$\Delta\sigma_{TOT}$ = 2.1 μb
d)
$q_i\ \bar{q}_i \rightarrow q_j\ \bar{q}_j$ (i≠j)
$\Delta\sigma_{TOT}$ = 3.9 μb
e)
$q_i\ q_i \rightarrow q_i\ q_i$ +
$q_i\ \bar{q}_i \rightarrow q_i\ \bar{q}_i$ +
$q_i\ \bar{q}_i \rightarrow gg$
$\Delta\sigma_{TOT}$ = -1.08 μb
$\frac{d\sigma}{dp_T}\left|_{\bar{p}p} - \frac{d\sigma}{dp_T}\right|_{pp}$ (μb/GeV/c)

Fig. 5